

Low-Frequency Sound Attenuation in the Deep Ocean

R. J. Urick

Citation: [The Journal of the Acoustical Society of America](#) **35**, 1413 (1963); doi: 10.1121/1.1918705

View online: <https://doi.org/10.1121/1.1918705>

View Table of Contents: <http://asa.scitation.org/toc/jas/35/9>

Published by the [Acoustical Society of America](#)

Articles you may be interested in

[Ray and Wave Invariants for SOFAR Channel Propagation](#)

The Journal of the Acoustical Society of America **46**, 1259 (1969); 10.1121/1.1911850

[Low-frequency ambient noise in the deep sound channel—The missing component](#)

The Journal of the Acoustical Society of America **69**, 1009 (1981); 10.1121/1.385680

[Transmission Characteristics of the SOFAR Channel](#)

The Journal of the Acoustical Society of America **48**, 767 (1970); 10.1121/1.1912201

[Sound channel in an exponentially stratified ocean, with application to SOFAR](#)

The Journal of the Acoustical Society of America **55**, 220 (1974); 10.1121/1.1914492

[Deep-Ocean Sound Attenuation in the Sub- and Low-Kilocycle-per-Second Region](#)

The Journal of the Acoustical Society of America **38**, 648 (1965); 10.1121/1.1909768

[Analytic Description of the Low-Frequency Attenuation Coefficient](#)

The Journal of the Acoustical Society of America **42**, 270 (1967); 10.1121/1.1910566

Low-Frequency Sound Attenuation in the Deep Ocean

R. J. URICK

U. S. Naval Ordnance Laboratory, White Oak, Silver Spring, Maryland

(Received 24 May 1963)

Signals received from Sofar bombs dropped from an aircraft eastward from Bermuda have been studied quantitatively. The energy density of the signals received at Bermuda, measured in various bands between 20 and 1600 cps, can be accounted for by cylindrical spreading beyond a "transition range" predicted approximately by simple considerations, plus an attenuation coefficient in dB per megayard given by the linear expression $1.5+8.2 f$, where f is the frequency in kc/sec. At frequencies below 1 kc/sec, this attenuation is far in excess of that which would be produced by absorption alone. At very low frequencies the excess attenuation is postulated to be due to the failure of the Sofar sound channel to act as an acoustic trap. At frequencies from about 50 to 500 cps, quantitative evidence is presented to indicate that the dominant attenuation process is scattering by index-of-refraction inhomogeneities deep in the sea. Other characteristics of Sofar-transmitted signals are described.

INTRODUCTION

IN the deep ocean, far from effects of the bounding surfaces, the attenuation of sound at frequencies below 1 kc/sec is known to be of the order of only a small fraction of a decibel per mile. For example, the formula $\alpha=0.033f^3$ (α in dB per kiloyard, f in kc/sec) proposed by Sheehy and Halley,¹ as a fit to their measurements, would indicate a coefficient of only 0.033 dB per kiloyard at 1 kc/sec, with smaller values at lower frequencies. Measurements of values as low as these require propagation paths that are measured in hundreds of miles, under conditions where reflection and scattering from the sea surface and sea bed are not involved. This implies, in turn, the use of the Sofar channel for long-distance propagation, since the required path lengths and freedom from boundaries cannot otherwise be obtained. In addition, the use of explosives is dictated by the need for high acoustic source levels.

The existence of a sound channel in the deep sea was predicted and demonstrated by Ewing and Worzel² about 20 years ago. Named for its use for sound fixing and ranging, it has received attention as a means of location of downed aviators and, more recently, of missile impacts.³ In consequence, the travel times for Sofar channel propagation have received abundant at-

ention.^{4,5} However, the amplitude, duration, and spectral characteristics of Sofar signals have not been studied extensively from a quantitative viewpoint, even though these characteristics are of dominant interest for long-range acoustic communication in the deep sea.

This paper describes the results of a series of measurements made across the Atlantic Ocean between Bermuda and the United Kingdom. The spreading law and attenuation coefficient for this series of shots and the loss produced by the Mid-Atlantic Ridge are described, and processes are postulated to account for the excess attenuation over that due to absorption at low frequencies.

MEASUREMENT PROCEDURE

Standard Navy Sofar signals, containing the equivalent of 4 pounds of TNT, were dropped on a pre-assigned time schedule by an aircraft as it flew between Bermuda and Great Britain via the Azores during June 1962. The location of the drops is shown in Fig. 1. The maximum range, from Bermuda to the furthest drop, was 2516 miles. At each location a pair of signals set to detonate at depths of 1500 and 3500 ft was dropped along with a sonobuoy for observing the instant of detonation aboard the aircraft. At the Bermuda end, recordings were made with hydrophones

¹ M. J. Sheehy and R. Halley, *J. Acoust. Soc. Am.* **29**, 464 (1957).

² M. Ewing and J. L. Worzel, *Geol. Soc. Am. Mem.* **27** (1948).

³ H. H. Baker, *Bell Lab. Record* **39**, No. 6, 195 (June 1961).

⁴ R. A. Frosch, M. Klerer, and L. Tyson, *J. Acoust. Soc. Am.* **33**, 1804 (1961).

⁵ G. M. Bryan, M. Truchan, and J. Ewing, *J. Acoust. Soc. Am.* **35**, 273 (1963).

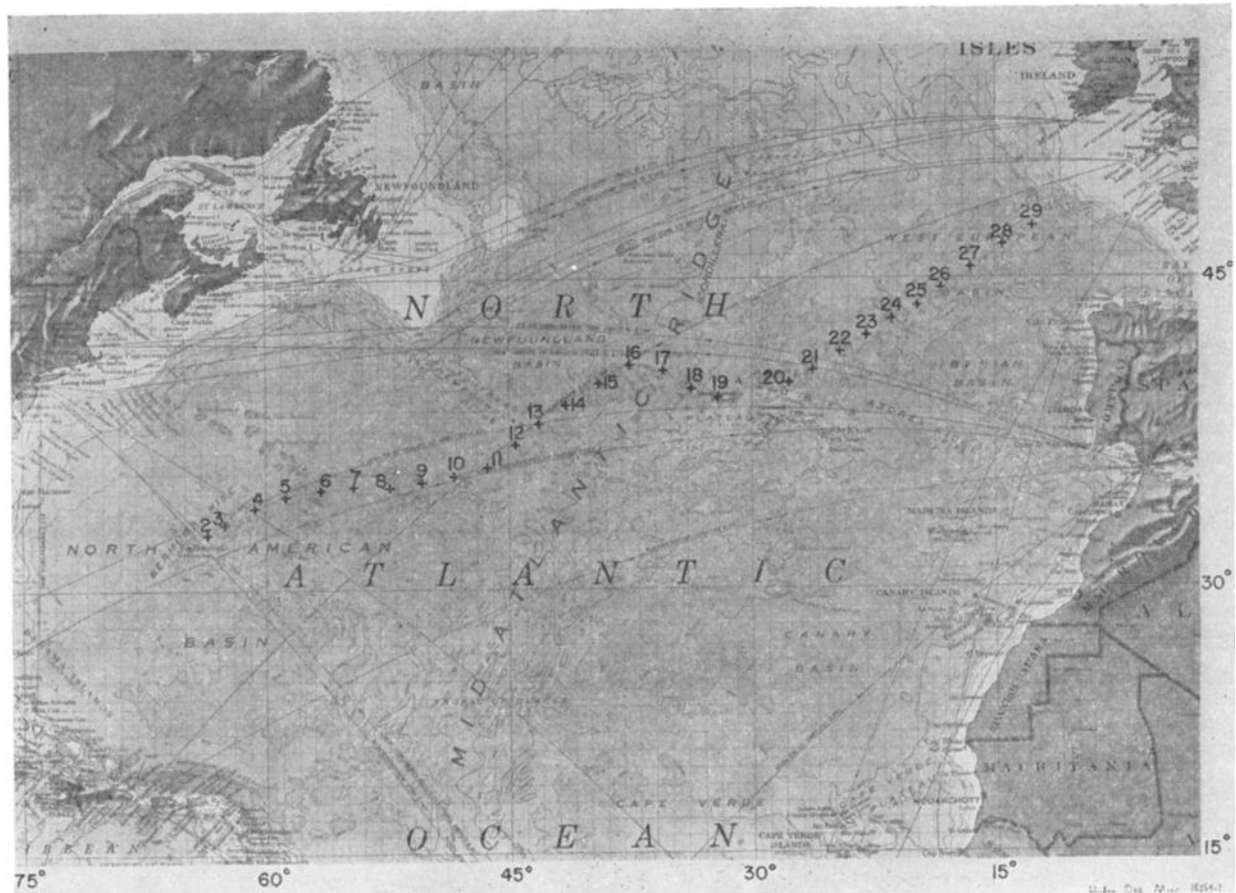


FIG. 1. Location of Sofar bomb drops.

at various depths; however, only the data from a hydrophone at 3900 ft, in water 14 000 ft deep, are described in this paper. The tape recordings were later analyzed in the conventional way by playing back into bandpass filters, squaring, and integrating to obtain the energy density of the received signals in the various filter bands.

SOFAR CHANNEL AND SIGNAL ENVELOPES

The Sofar sound channel is an internal acoustic duct having its axis, or depth of minimum velocity, at depths ranging from about 5000 ft in the tropics to near the surface in high latitudes. Its existence depends upon the fact that the velocity of sound increases with both temperature and pressure; at shallow depths, where the temperature decreases with depth, the temperature effect is dominant and the velocity decreases; at great depths where the sea is nearly isothermal, the pressure effect causes the velocity to increase again. Figure 2, taken from the now-classic paper on the subject by Ewing and Worzel,² shows a typical velocity profile in midlatitudes, together with a ray diagram for a source on the axis. Ray paths near the axis carry most of the energy and are associated with the longest travel time.

As a result, Sofar signals received at a great distance have a typical envelope that shows a gradual buildup and reaches a sudden climax at the instant that the axially traveling energy arrives. This abrupt ending is the characteristic that makes them useful for triangulation purposes.

Along the path of the drops shown in Fig. 1, the transmission of sound in the Sofar channel is interrupted by the Mid-Atlantic Ridge, which forms an acoustic barrier for deep propagation across the Atlantic Ocean. Bathymetric charts⁶ show numerous places in the vicinity of the acoustic path where the crests of the Ridge pierce the depth of the Sofar axis and thus cut off near-axial rays carrying the principal portion of the transmitted energy. The attenuating effect of the Ridge will be evident in the results to follow; in spite of it, signals were received 5 to 10 dB above noise at the maximum range (Drop 29), although the drops just beyond the Ridge (Drops 20, 21) appear to have been cut off by the shadowing effect of the crests and were not received at Bermuda.

The sound-velocity structure along the line of drops

⁶ Charts BC 0307N, BC 0308N, published by the U. S. Navy Oceanographic Office.

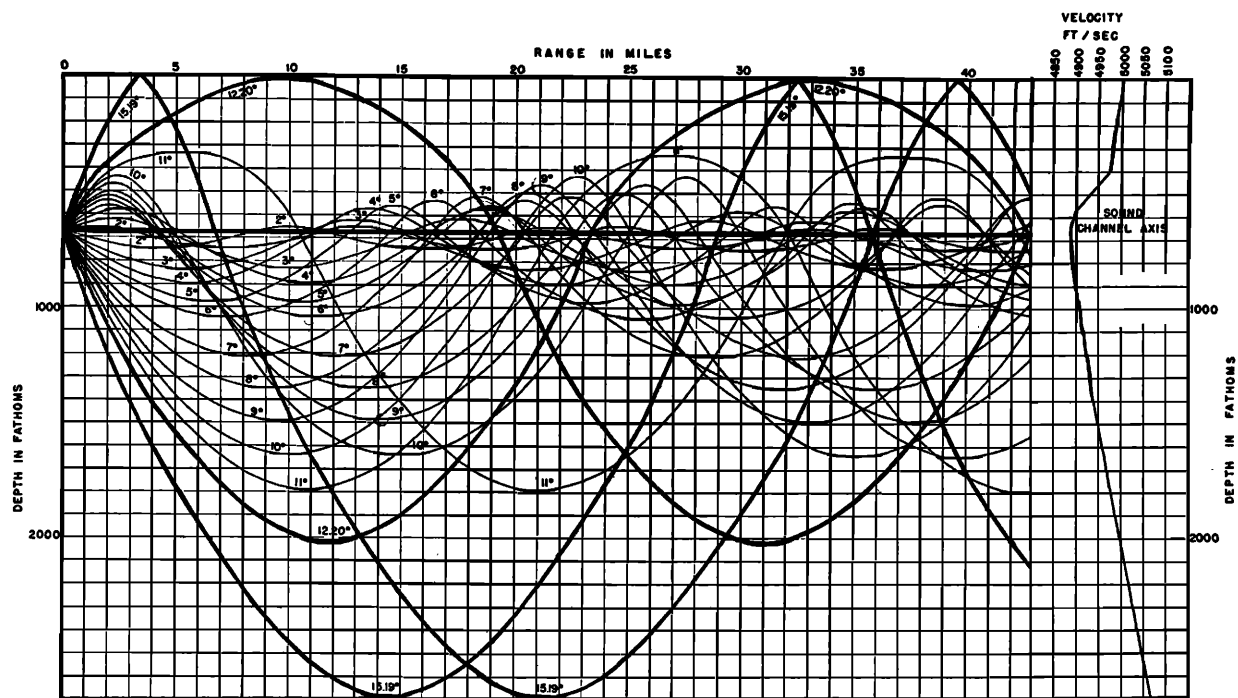


FIG. 2. Ray diagram of the Sofar sound channel. [Reproduced from Ewing and Worzel.²]

was estimated from velocity data provided by the National Oceanographic Data Center. Figure 3 is a velocity contour cross section drawn from N.O.D.C. hydrographic data for the month of June at stations in the vicinity of the drop path. The feature most worthy of note is the decreasing velocity at shallow depths toward the right, reflecting the lower surface temperatures toward the northeast along the drop path. However, the depth of the Sofar axis is approximately constant, although at the northeasterly end its depth is made uncertain by the occurrence of nearly isovelocity conditions.

Figure 4 shows signal envelopes in the band 50–150 cps for a shot at 3500 ft as received by the hydrophone at 3900 ft at Bermuda. The vertical scale shows the band level in decibels relative to the intensity of a plane wave of 1 dyn/cm² rms pressure. The envelopes exhibit the expected lengthening and weakening with increasing range. Signals from drops on the far (eastern) side of the Mid-Atlantic Ridge were weaker and shorter than those on the near side, presumably because of the removal of near-axial rays by the Ridge. In no case beyond Drop 3 (93 miles) did the signals exhibit a clear beginning.

Figure 5 is a plot of signal duration against range, using two criteria for measurement of duration. If the signal duration is taken to be the interval from a point on the envelope 3 dB above the ambient noise background to the sudden termination, the duration shows a steady increase with range out to the Ridge. By simple ray theory for a linear gradient, it can be shown, as has

been done by Brekhovskikh,⁷ that for both source and receiver on the axis of a sound channel the difference in travel times along the axial ray and along the ray leaving the source at an angle θ_0 is $t\theta_0^2/6$, where t is the axial travel time. The straight line in Fig. 5 shows this calculated duration for $\theta_0=12.2^\circ$ for the ray of maximum inclination propagating without reflection at either the sea surface or sea bed. The agreement is surprising, considering that the Sofar channel has by no means the linear gradient on either side of its axis required for this approximation. The absence of a clear beginning to the received signal is perhaps due to the contribution by rays which leave the source beyond 12.2° and which suffer repeated reflection at either or both sea boundaries. Beyond the Ridge at about a range of 1800 miles, the durations based on the above criterion are much shorter because the early portion of the signals are buried in noise, and because the near-axial rays are cut off by the Ridge. In the South Atlantic, where the Ridge crests do not pierce the Sofar axis, the effect of the Ridge on signal duration is not as great.⁵ If, however, one measures from a point on the envelope 1 Np (8.7 dB) below the peak intensity to the cessation of the signal, a steady increase along the whole path is found, as indicated in the right-hand portion of Fig. 5. If the envelope be assumed exponential, the convenience of this criterion is that the energy level E can easily be shown to be related to the peak intensity level

⁷L. M. Brekhovskikh, *Waves in Layered Media* (Academic Press Inc., New York, 1960), Eq. 39.14.

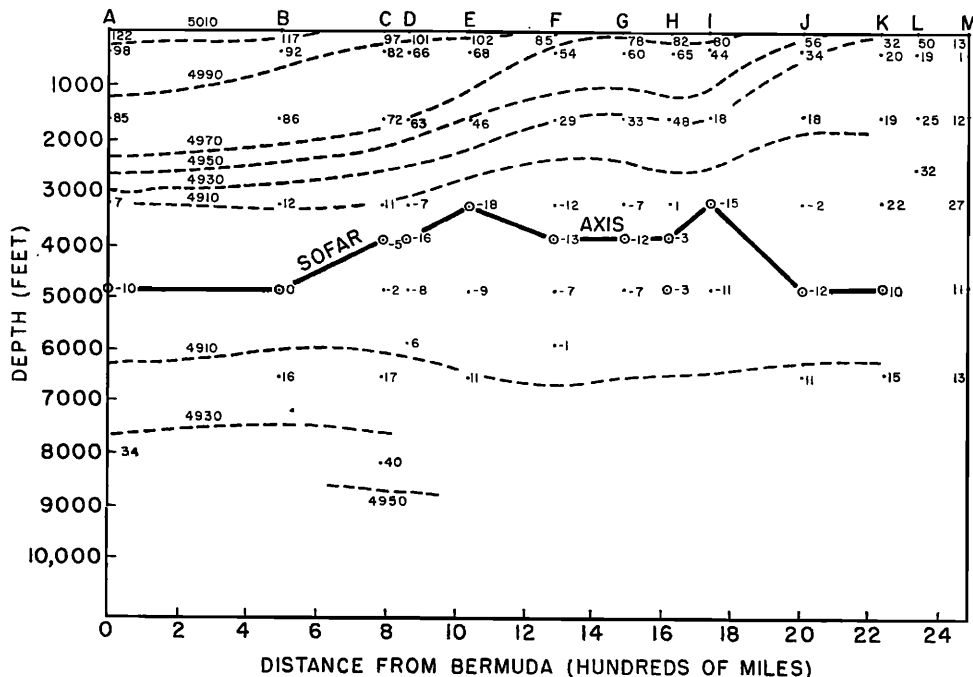


FIG. 3. Velocity structure along a profile approximating the path flown. Velocity data at selected oceanographic stations during the month of June, as compiled and computed by the National Oceanographic Data Center from measured temperature and salinity data, using the Kuwahara formula. Velocity values in ft/sec relative to 4900 ft/sec (i.e., 4900 ft/sec=0). Minimum values (circled), shown at tabulated depths for the various observation stations, determine the depth of the Sofar axis. Locations of various stations A to M are:

A: 32°1N, 64°5W;	B: 38.5N, 56.7W;	C: 38.0N, 50.2W;
D: 37.2N, 48.5W;	E: 36.1N, 44.0W;	F: 37.1N, 38.1W;
G: 39.5N, 33.7W;	H: 39.9N, 31.1W;	I: 41.1N, 29.8W;
J: 43.6N, 24.1W;	K: 43.1N, 18.1W;	L: 45.0N, 16.0W;
M: 48.1N, 12.7W.		

I and the above interval T_2 in seconds by the simple relationship $E=I+10 \log T_2-3$, where E is in decibels referred to the unit of intensity, taken for a period of 1 sec.

against range for shots at 3500- and 1500-ft depths. The shots at 1500 ft were about 10 dB weaker than those near the axis of the Sofar channel. The dashed curves

PREDICTED MAXIMUM RANGE

Figure 6 is a plot of the peak-signal intensities read from the signal envelopes in the 50- to 150-cps band

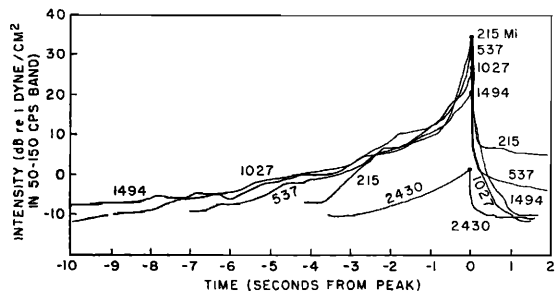


FIG. 4. Rectified envelope of received signals at various ranges. The signal at 2430 miles came from a shot on the east side of the Mid-Atlantic Ridge. The traces shown are from Drops 4, 7, 12, 17, and 28 (Fig. 1).

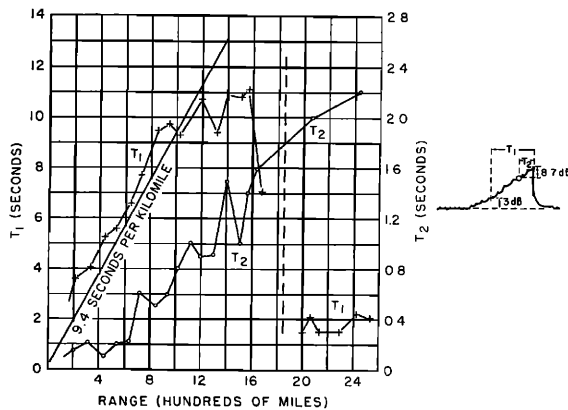


FIG. 5. Signal durations in the 50- to 150-cps bands from a point on the rectified envelope 3 dB above ambient noise to the end of the signal (crosses) (T_1), and from a point 8.7 dB below the peak signal to the end (circles) (T_2). The vertical dashed line is at the location of the Mid-Atlantic Ridge. The sloping line is the prediction based on a linear velocity gradient. Different scales are used for T_1 and T_2 .

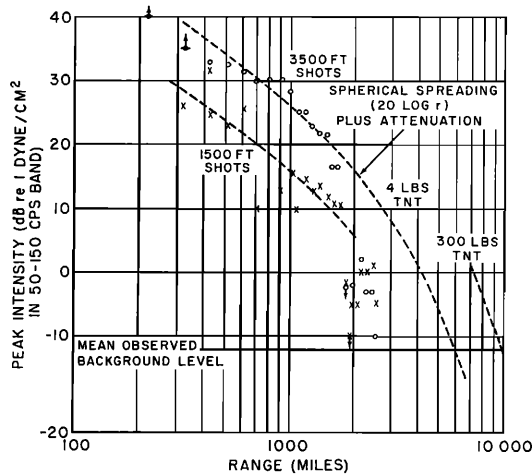


FIG. 6. Peak Sofar signal intensities in the 50- to 150-cps band for shots at 1500 and 3500 ft. The dashed curves show spherical spreading plus attenuation at 4.0 dB per kilometer. The extrapolated peak level equals the mean ambient level at 6000 miles for a 4-lb charge as used in the experiment. The signal from a 300-lb depth charge would equal ambient at 10 000 miles.

show spherical spreading⁸ plus attenuation fitted to the measured data and (for the 3500-ft shots) extrapolated in range until the measured average level of the ambient background is reached. If this can be taken as the limit of detectability, then a 4-lb charge should be received out to a range of 6000 miles, and a 300-lb charge to about 10 000 miles, in the absence of attenuation caused by a major path obstruction such as the Mid-Atlantic Ridge in the vicinity of the Azores. The latter distance may be compared with the observation made by the Lamont Geological Observatory⁹ that a depth charge detonated off the coast of Australia was heard at Bermuda 12 000 miles away.

ENERGY ANALYSIS

The signals whose envelopes have just been described were filtered in octave and third-octave bands and integrated so as to obtain energy density. In the following, the unit of energy density is the energy density of a plane wave of rms pressure 1 dyn/cm² taken for a period of 1 sec; in decibel units, this reference is abbreviated simply as 1 dyn/cm², in analogy with the practice for intensity. Figures 7 and 8 show measured values of a single drop in various bands of the quantity $E + 10 \log r$, where E is the band energy density in dB relative to 1 dyn/cm² and r is the range in yards. Thus, these values are energy-density "corrected" for cylin-

⁸ Although energy spreads cylindrically in a channel, intensity must decrease as the inverse square of the distance in the Sofar channel because of the travel time dispersion discussed above. In the recently reported work of Bryan, Truchan, and Ewing,⁵ an inverse third power, instead of inverse square, is said to fit the measured peak intensities. However, attenuation, in the unspecified filter band used, was neglected; inverse-cube spreading may well be sensibly equivalent to inverse-square spreading plus attenuation.

⁹ Note, Trans. Am. Geophys. Union 41, 670 (1960).

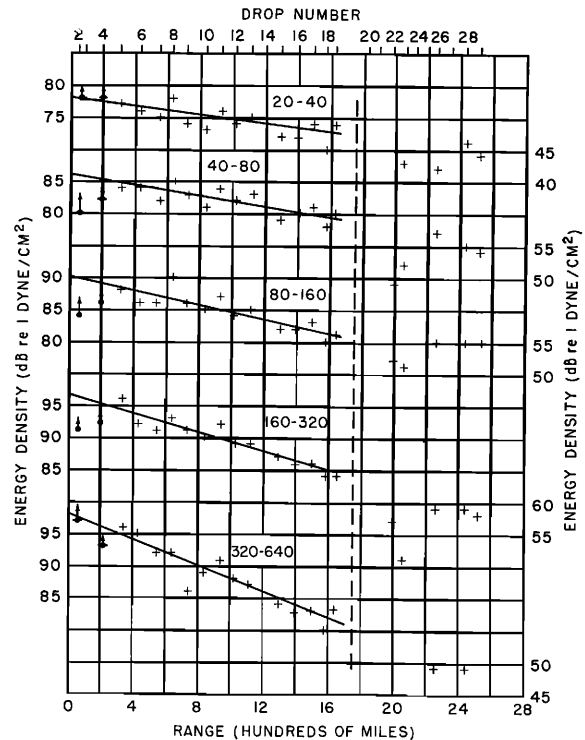


FIG. 7. Energy density levels plus $10 \log r$, in units of dB relative to the energy density of a 1-dyn/cm² plane wave for a period of 1 sec (dB re 1 dyn/cm²) in octave bands. The vertical dashed line shows location of Mid-Atlantic Ridge. Different level scales are used for the data on each side of the ridge.

drical spreading. The fit of the data to the straight lines drawn by eye through the plotted points indicates that the decrease in energy density with range may be described in terms of cylindrical spreading ($10 \log r$) plus an attenuation loss proportional to range. Thus, the energy density level E_r at range r in yards can therefore be related to the energy density level E_0 at the unit range of 1 yard by the expression

$$E_r = E_0 - 20 \log r_0 - 10 \log(r/r_0) - \alpha r \times 10^{-6} \\ = (E_0 - 10 \log r_0) - 10 \log r - \alpha r \times 10^{-6},$$

where r_0 is a transition range separating the regions of spherical and cylindrical spreading, and α is an attenuation coefficient measured in dB per megayard (10^6 yards). In Figs. 7 and 8, the intercept at zero range is the quantity $E_0 - 10 \log r_0$, while the slope is the coefficient α . Table I lists measured values for $(E_0 - 10 \log r_0)$, α , and the energy loss produced by the Mid-Atlantic Ridge for the various analysis bands.

EXPLOSIVE SOURCE LEVELS

Further analysis requires a determination of E_0 , the source energy density level at 1 yard. In order to obtain this quantity, 4-lb Sofar bombs similar to those used

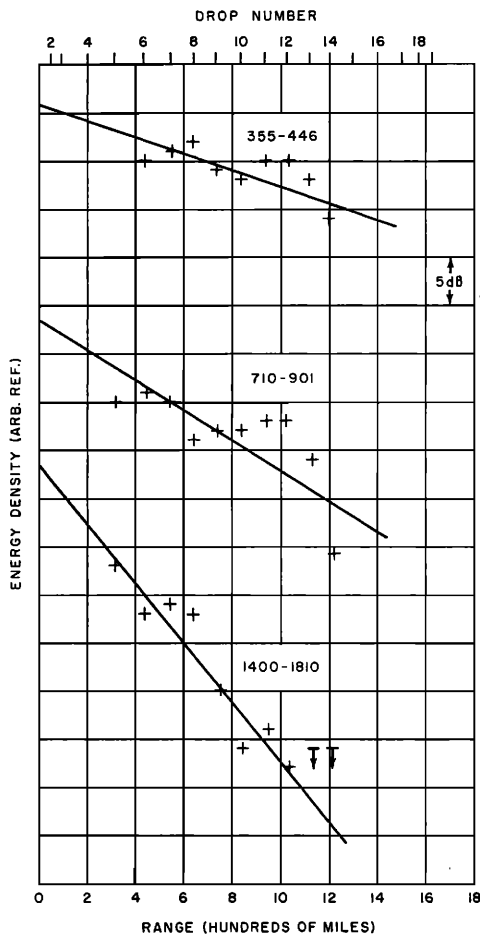


FIG. 8. Energy density levels plus $10 \log r$ in third-octave bands. Relative scale only.

aboard the aircraft were dropped from a surface ship, and the detonation was recorded with a hydrophone at a depth of 300 ft. The tape-recorder signal was later analyzed digitally. Only the shockwave and first bubble

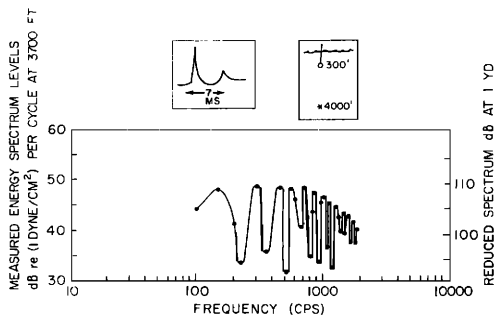


FIG. 9. Energy-density spectrum of a 4-lb Sofar bomb detonated at 4000 ft and measured at 300 ft, as obtained by digital analyses of the pressure-time curve. The scale at right shows reduced levels at 1 yard obtained by assuming spherical spreading ($20 \log 3700/3$). The mean spectrum was used for computing octave and third-octave band levels.

pulse, occurring at the expected¹⁰ interval of 7 msec after the shockwave for the particular charge weight and depth used, were found to make an appreciable contribution to the total energy. Figure 9 shows energy spectrum levels at the measurement distance of 3700 ft, obtained by digital analysis at frequency intervals of 50 cps. The right-hand scale gives these levels reduced to one yard on the assumption that spherical spreading applies to the shockwave as well as to the bubble-pulse contribution. This assumption yields one-yard levels different from those which would be actually measured at 1 yard, inasmuch as the scaling laws for shockwaves are ignored; the corrections required would lie between 0 and 5 dB, depending on frequency. The measured data agree well with the spectra reported by Weston.¹¹ From this spectrum, octave and third-octave band levels were computed, and are given in Table I.

TABLE I. Transition range, attenuation coefficient, and Mid-Atlantic Ridge loss in various frequency bands.

Freq. band, cps	Mid-freq.	$(E_0 - 10 \log r_0)$	α	Energy loss across Mid-Atlantic Ridge	E_0	$10 \log r_0$	r_0 yards
20-40	28	78 dB	1.7	25 dB	113 dB	35	3000
40-80	56	86	2.2	21	120	34	2500
80-160	110	90	2.8	22	126	36	4000
160-320	220	97	3.7	20	129	32	1600
320-640	450	98	5.0	25	132	34	2500
355-446	400	...	4.5
710-901	790	...	7.8
1400-1810	1590	...	15.6

TRANSITION RANGE

Corresponding values for the transition range r_0 for various filter bands are also given in Table I. They range from 1600 to 4000 yards. Although these ranges may be thought to be surprisingly small when compared with the scale of the ray diagram of Fig. 2, it should be remembered that most of the energy is carried by rays that remain relatively near the channel axis and cross it at relatively short-range intervals.

A theoretical estimate of the transition range can be made by assuming that the energy within a small ray bundle becomes, at a sufficiently long range, distributed uniformly over the channel width that it occupies. Thus, in Fig. 10, the energy emitted by the source within the small angle $\Delta\theta$ is assumed to be spread over its track width H at a sufficiently long-range r . As shown in the Appendix, this leads to the simple expression

$$(r_0)_k = H / \Delta\theta \cos\theta$$

for the transition range of the k th bundle, so that the

¹⁰ R. H. Cole, *Underwater Explosions* (Princeton University Press, Princeton, New Jersey, 1948), Sec. 8.3.

¹¹ D. E. Weston, *Proc. Phys. Soc.* **76**, 233 (1960).

transition range r_0 for all the trapped energy is given by

$$1/r_0 = \sum_k 1/(r_0)_k,$$

where the summation is taken over all bundles that are trapped in the channel.

This summation process was carried out for the velocity profile at Bermuda (Location A, Fig. 3), extrapolated downward at the rate of 0.0164 ft/sec/ft according to Wilson's formula.¹² The profile was divided into increments of 10 ft/sec, H was measured, and the corresponding values of θ were computed by Snell's law for a source on the axis. The resulting value for the transition range was 5900 yards. This agrees with the measured values as well as could be expected, considering the crudeness of the basic assumption and the above-mentioned uncertainty in source level.

ATTENUATION

The attenuation coefficients of Table I are plotted against frequency in Fig. 11, and can be fitted within the limits of accuracy of their determination by the

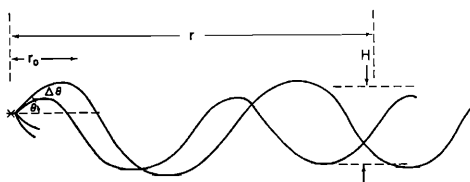


FIG. 10. The energy within a small ray bundle $\Delta\theta$ is assumed to be distributed uniformly over the channel thickness H at a sufficiently long-range r . This assumption enables the transition range r_0 , separating the regions of spherical and cylindrical spreading, to be computed.

linear expression

$$\alpha = 1.5 + 8.2f,$$

where α is expressed in dB per megayard, and f is the frequency in kilocycles per second. It should be pointed out, in passing, that the measured attenuation coefficients do not depend on the absolute calibration of the measurement system, the source level, or the transition range, since they are merely the slopes of energy level vs range plots when adjusted for spreading.

The measured coefficients are seen to be higher by an order of magnitude than the attenuation that would be produced by absorption alone.¹³ An excess attenuation in deep-sea transmission over what would be produced by absorption was also found by Sheehy and Halley,¹ as is evidenced by their empirical formula $\alpha = 33f^{3/2}$ (α in dB/megayard, f in kc/sec). The Sheehy-Halley method of determining attenuation, however, was a differential method yielding only relative values

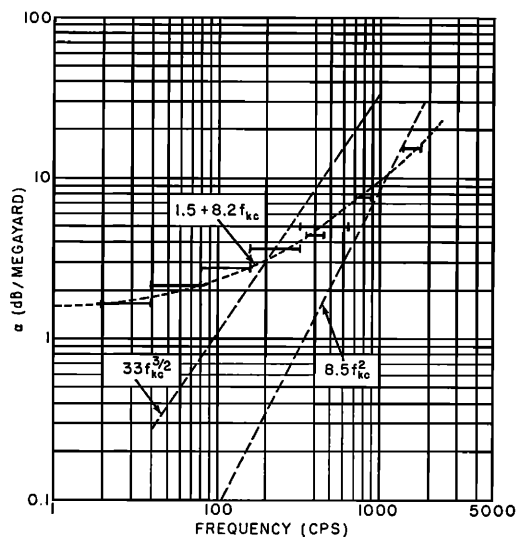


FIG. 11. Measured attenuation in units of dB per megayard (=500 miles), plotted over the bandwidths used. The values are fitted approximately by the linear expression $\alpha = 1.5 + 8.2 f$, where f is in kc/sec. The sloping lines are for $\alpha = 33 f^{3/2}$ as reported by Sheehy and Halley,¹ and for $\alpha = 8.5 f^2$ expected from absorption alone.

for the coefficient. The expression just cited fitted the measured data when zero attenuation was assumed at 40 cps; the present determination yields a value of 1.8 dB/megayard at this frequency. In Fig. 12 are plotted the Sheehy-Halley coefficients adjusted to 1.8 dB/megayard at 40 cps. The excellent agreement between the present data and the Sheehy-Halley coefficients adjusted in this way indicates a close compatibility between two experimental results, one of which was obtained in the Pacific and the other in the Atlantic Ocean Basin. Figure 11 shows that the coefficients obtained in the present experiment are much higher at frequencies below 100 cps than those predicted by the Sheehy-Halley formula.

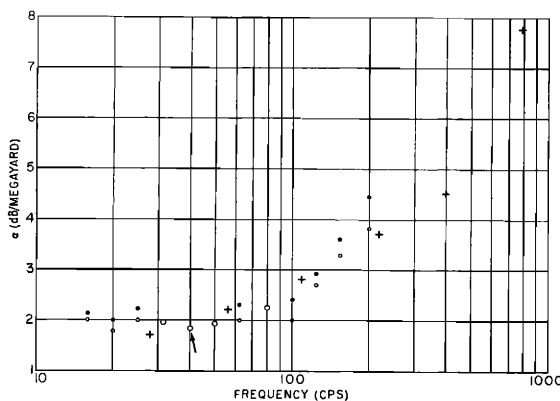


FIG. 12. Comparison with Sheehy-Halley results when the latter are adjusted to a value of 1.8 dB/my at 40 cps (instead of zero). Crosses: present data; dots and circles: Sheehy-Halley data from hydrophones at Kaneohe and Point Sur, respectively.

¹² W. D. Wilson, *J. Acoust. Soc. Am.* **32**, 641 (1960).

¹³ M. Schulkin and H. W. Marsh, *J. Acoust. Soc. Am.* **34**, 864 (1962).

CAUSES OF THE EXCESS ATTENUATION

A number of processes may be imagined to account for the excess attenuation over that due to absorption alone. Losses at the sea surface and sea bottom must be ruled out when both sources and receiver are near the axis since the bulk of the transmitted energy must travel at depths near the channel axis.

The most likely cause of attenuation for deep paths appears to be scattering by inhomogeneities in sound velocity lying at near-axial depths in the sea. These index-of-refraction inhomogeneities may be due to variations of temperature, salinity, or water currents along the deep propagation paths. These inhomogeneities will scatter transmitted sound into angles beyond the maximum inclination angle for rays trapped by the channel. Thus, referring to Fig. 13, a patch of inhomogeneity will scatter a portion of the energy of the incident-ray bundle $AA'-BB'$ into angles beyond the limits of the bundle (about $\pm 12^\circ$, near the Sofar axis) that will be lost to the channel.

Chernov¹⁴ gives expressions for the attenuation of a divergent-ray bundle produced by scattering beyond the boundaries of the bundle. If the scattering inhomogeneities have a spatial correlation function of the form $e^{-r/a}$, the attenuation coefficient is found to reduce to

$$\alpha = \frac{\langle 8\mu^2 \rangle (ka)^4}{a} \frac{1 - \sin^2 \theta_0 / 2}{(1 + 4y^2)(1 + 4y^2 \sin^2 \theta_0 / 2)},$$

and if the correlation function is of the form e^{-r^2/a^2} ,

$$\alpha = \frac{[(\pi)^{1/2} \langle \mu^2 \rangle y^2]}{a} (e^{-y^2 \sin^2 \theta_0 / 2} - e^{-y^2}),$$

where a is a correlation distance, sometimes called the "patch size" of the inhomogeneities; $\langle \mu^2 \rangle$ is the mean square index of refraction variation; $2\theta_0$ is the divergence angle of the bundle; $y = ka = 2\pi a / \lambda$, with λ the wavelength.

Figure 14 is a comparison of the measured attenuation with the theoretical attenuation using these expressions,

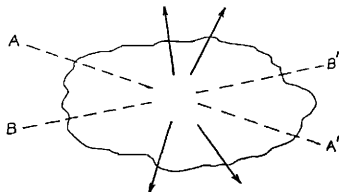


FIG. 13. Scattering at a patch of inhomogeneity of the ray bundle $AA'-BB'$ into angles that are not trapped in the Sofar channel.

¹⁴L. A. Chernov, *Wave Propagation in a Random Medium* (McGraw-Hill Book Company, Inc., New York, 1960), Eqs. 65 and 66.

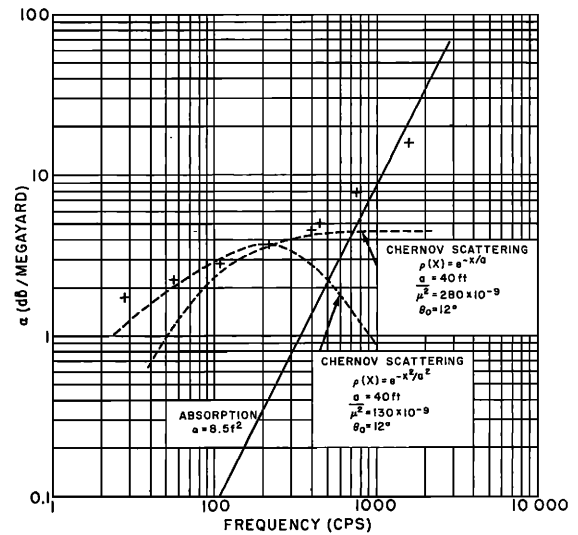


FIG. 14. Theoretical attenuation produced by scattering out of the Sofar channel for two correlation functions for the inhomogeneities, using formulas derived by Chernov.

for $a = 40 \text{ ft}$, $\langle \mu^2 \rangle = 280 \times 10^{-9}$ in the first case and $a = 40 \text{ ft}$, $\langle \mu^2 \rangle = 130 \times 10^{-9}$ in the second. With these values for the parameters, an acceptable fit to the measured attenuation coefficients is found.

It is of interest to compare these values of a and $\langle \mu^2 \rangle$ with those found by microthermal measurements at shallow depths by Lieberman¹⁵ ($a = 2 \text{ ft}$, $\langle \mu^2 \rangle = 5 \times 10^{-9}$) and Urick and Searfoss¹⁶ ($a = 150 \text{ ft}$, $\langle \mu^2 \rangle = 640 \times 10^{-9}$, below the mixed layer). The Kolmogorov ratio $\langle \mu^2 \rangle / a^{\frac{2}{3}}$, which by the Kolmogorov-Obukov theory of turbulent diffusion would be a constant under conditions of turbulent equilibrium,^{17,18} is found to lie within an order of magnitude for these microthermal measurements and for the acoustically derived data. In addition to suggesting the validity of the basic hypothesis, this agreement also indicates the existence of equilibrium in the turbulent exchange processes below the mixed layer, and extending down to appreciable depths in the sea. However, a different turbulent regime appears to be present within the mixed layer; the microthermal measurements in the mixed layer of Urick and Searfoss¹⁶ ($a = 150 \text{ ft}$, $\langle \mu^2 \rangle = 0.3 \times 10^{-9}$), and of Whitmarsh, Skudrzyk, and Urick,¹⁹ obtained with a bar along which thermal pickups were mounted ($a = 2.1 \text{ ft}$, $\langle \mu^2 \rangle = 0.02 \times 10^{-9}$; $a = 12\frac{1}{2} \text{ ft}$, $\langle \mu^2 \rangle = 0.066 \times 10^{-9}$), yield values for

¹⁵L. Lieberman, *J. Acoust. Soc. Am.* **23**, 563 (1951).

¹⁶R. J. Urick and C. W. Searfoss, "The Microstructure of the Ocean near Key West, Florida, Part II—Analysis," *Naval Res. Lab. Rept. S-3444* (April 1949).

¹⁷A. DeFant, *Physical Oceanography* (Pergamon Press, Inc., New York, 1961), Vol. 1, pp. 393-398.

¹⁸C. C. Lin, *Turbulent Flows and Heat Transfer* (Princeton University Press, Princeton, New Jersey, 1959), pp. 223-225.

¹⁹D. C. Whitmarsh, E. Skudrzyk, and R. J. Urick, *J. Acoust. Soc. Am.* **29**, 1124 (1957).

the ratio $\langle \mu^2 \rangle / a^2$ about two orders of magnitude smaller than those below the layer.

At the low end of the spectral range, the Sofar channel fails to trap sound of long wavelength, and the ocean begins to act as a coupling fluid between the sound source and the earth, rather than as an effective acoustic trap. Thus, at very low frequencies, the attenuation should begin to increase with decreasing frequency as fewer and fewer modes remain trapped. A suggestion that this is happening may be seen in the Sheehy-Halley data below 40 cps (Fig. 12).

An expression for the lowest trapped frequency for radio waves in atmospheric ducts may be taken over bodily for the corresponding underwater analog. When the axis of the duct lies at a depth d , the longest wavelength trapped is that which just "fits" in the duct between the axis and the surface, and can be shown to be approximately²⁰

$$\lambda_{\max} = 8/3(2)^{\frac{1}{2}} \int_0^d [N(d) - N(z)]^{\frac{1}{2}} dz,$$

where $N(z)$ is the index of refraction at depth z , and $N(d)$ is the index of refraction on the duct axis.

If for simplicity we assume a linear gradient g for the index of refraction above the axis, such that for $z < d$

$$N(d) - N(z) = g(d - z),$$

and carry out the integration, the result is

$$\begin{aligned} \lambda_{\max} &= (16/9)(2)^{\frac{1}{2}}(gd)^{\frac{1}{2}} \cdot d \\ &= (16/9)(2)^{\frac{1}{2}}(\Delta V/V)^{\frac{1}{2}} \cdot d, \end{aligned}$$

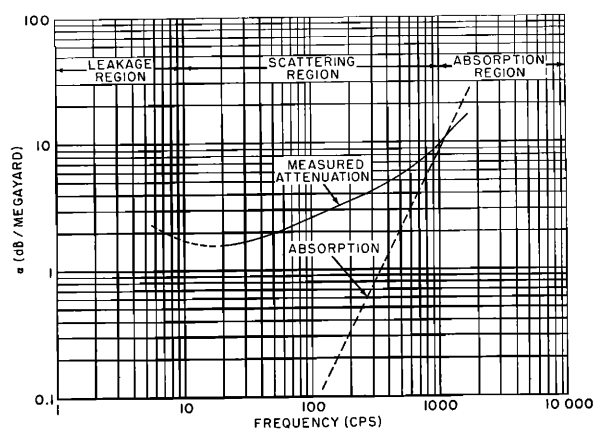


FIG. 15. Attenuation regions for Sofar transmission. Three regions are postulated, in which the attenuation-producing processes are those of leakage, scattering, and absorption.

where ΔV is the change in sound velocity between the axis and the surface, and V is the axial velocity. Using values for ΔV , V , and d from Fig. 3, we find $\lambda_{\max} = 2000$ and 1400 ft at Bermuda and at the Azores. Thus, frequencies of the order of 2.3 and 3.5 cps are predicted to be the lowest frequencies trapped in the Sofar channel; at such frequencies, where the first mode begins to be leaky, a relatively high attenuation should exist.

CONCLUSIONS

In summary, three processes for the attenuation in Sofar propagation, when both source and receiver lie near the channel axis, may be postulated (Fig. 15). Below 10 cps the dominant source of attenuation is probably leakage out of the Sofar channel so that low frequencies fail to be trapped in the channel; between about 10 and 1000 cps, the attenuation is probably due to scattering by inhomogeneities lying near the channel axis; above 1000 cps, the dominant attenuation process is the conversion of acoustic energy to heat by absorption.

ACKNOWLEDGMENTS

The author is indebted to many groups and individuals for assistance in the work just described. Special thanks are due to A. E. Adams and the flight personnel of the Naval Air Test Center, Patuxent, Maryland, and to Dr. W. A. VonWinkle and others of the Trident Laboratory, Bermuda, for obtaining the field data; to R. Richter of Daystrom, Inc., for obtaining and analyzing the explosive source level data; to G. Lund of NOL for assistance in analysis; and to T. F. Johnston and C. B. Brown of NOL for many helpful discussions.

APPENDIX

Referring to Fig. 10, consider a pair of rays having inclination angles of $\theta - (\Delta\theta/2)$ and $\theta + (\Delta\theta/2)$ at the source. At a distance of 1 yard from the source, this pair of rays subtends an area $2\pi\Delta\theta \cos\theta$. If the energy density of the source at one yard is E_0 , the acoustic energy radiated into $\Delta\theta$ becomes $2\pi E_0 \Delta\theta \cos\theta$. At a long range r , this energy is postulated to be evenly distributed throughout the channel thickness H , and thus will be spread over an area $2\pi r H$. Hence, the energy density ΔE_r at r , contributed by the energy radiated into $\Delta\theta$, is then $2\pi E_0 \Delta\theta (\cos\theta) / 2\pi r H$, or

$$\begin{aligned} \Delta E_r &= (E_0 \Delta\theta \cos\theta) / r H \\ &= E_0 / r r_0', \end{aligned}$$

²⁰ D. E. Kerr, *Propagation of Short Radio Waves* (McGraw-Hill Book Company, Inc., New York, 1951), pp. 18-21.

if we write

$$r_0' = H / \Delta\theta \cos\theta$$

for the transition range r_0' for the ray bundle $\Delta\theta$. At a point on the axis of the channel, the total energy density is the sum of all the contributions $\Delta\theta$ out to the limit of θ set by the channel. If the transition range of the k th contribution be denoted as $(r_0)_k$, then the total energy

density is

$$E_r = \sum_k \Delta E_r = \frac{E_0}{r} \sum_k \frac{1}{(r_0)_k} = \frac{E_0}{r} \cdot \frac{1}{r_0},$$

where r_0 is the effective transition range for the channel as a whole.